

# 11. Shape and intrusion history of the Late Caledonian Newry Igneous Complex, Northern Ireland

MARK COOPER,<sup>1</sup> PAUL ANDERSON,<sup>2</sup> DANIEL CONDON,<sup>3</sup> CARL STEVENSON,<sup>2</sup> ROB ELLAM,<sup>4</sup> IAN MEIGHAN<sup>1</sup> AND QUENTIN CROWLEY<sup>5</sup>

How to cite this chapter:

Cooper, M.R., Anderson, P., Condon, D.J., Stevenson, C.T.E., Ellam, R.M., Meighan, I.G. and Crowley, Q.G., 2016 'Shape and intrusion history of the Late Caledonian, Newry Igneous Complex, Northern Ireland' in M.E. Young (ed.), *Unearthed: impacts of the Tellus surveys of the north of Ireland*. Dublin. Royal Irish Academy.

DOI:10.3318/  
978-1-908996-88-6.ch11

The Tellus high-resolution airborne magnetic and radiometric maps define previously unmapped zones within the Newry Igneous Complex, County Down. High-precision uranium–lead zircon dating of nine rock samples from different parts of the complex provides a robust set of age constraints (*c.*414–407 Ma), which confirm that the different plutons of the complex young towards the south-west. Combined, these new data allow an innovative model of intrusion to be developed, with intrusion beginning in the north-east and progressing towards the south-west.

## INTRODUCTION

The Late Caledonian Newry Igneous Complex was intruded into the Southern Uplands – Down–Longford terrane after closure of the Iapetus Ocean (Cooper and Johnston, 2004a). It belongs to a group of plutons and complexes referred to as the 'Newer Granites' suite that was intruded into northern Britain and Ireland between 435 and 380 million years ago (Brown *et al.*, 2008). A number of these 'Newer Granites' are found within the Southern Uplands – Down–Longford terrane and include the Crossdoney pluton in the Republic of Ireland and the Loch Doon pluton in south-west Scotland, both of which are located in the Northern Belt north of the Orlock Bridge Fault. South of the Orlock Bridge Fault in the Central Belt in south-west Scotland occur the Fleet and Criffel plutons (Fig. 11.1a).

Work to date has shown the Newry Igneous Complex to be composed of three granodioritic plutons with smaller, intermediate-ultramafic bodies at its north-east end (Meighan

<sup>1</sup> Geological Survey of Northern Ireland, Belfast.

<sup>2</sup> University of Birmingham.

<sup>3</sup> British Geological Survey, Keyworth.

<sup>4</sup> Scottish Universities Environmental Research Centre, East Kilbride.

<sup>5</sup> Trinity College, Dublin.

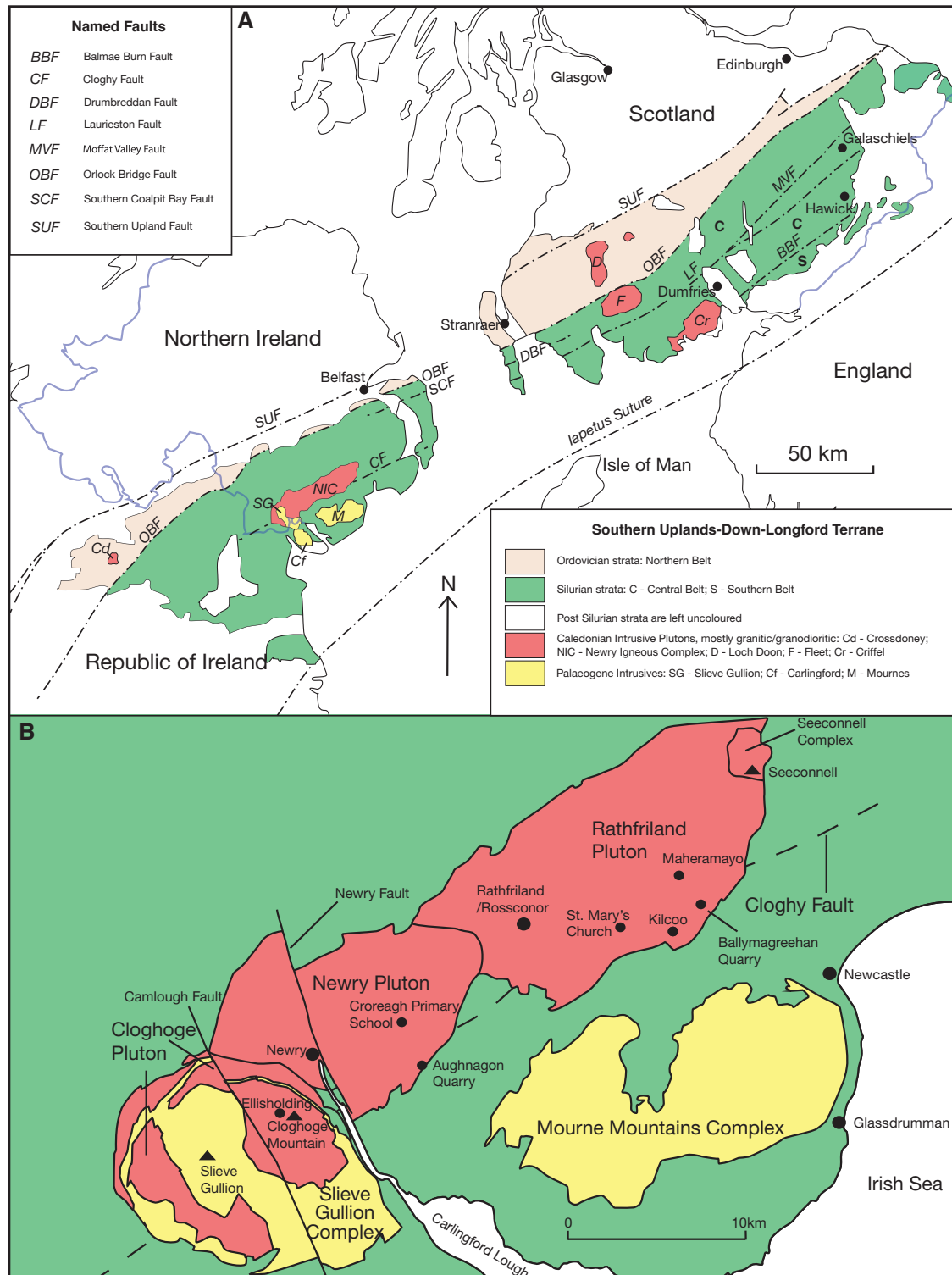


Figure 11.1 (a) The Southern Uplands – Down–Longford terrane showing locations of the main Late Caledonian intrusions relative to major faults and the Iapetus Suture (redrawn from Beamish *et al.*, 2010). (b) Detailed map of the Newry Igneous Complex (after GSNI, 1997; Cooper and Johnston, 2004a).

and Neeson, 1979; Neeson, 1984). The main plutons, previously termed the Northeast, Central and Southwest, are renamed here as the Rathfriland, Newry and Cloghoge respectively (Fig. 11.1b). Based on field relationships (Meighan and Neeson, 1979) the intrusions are known to young from north-east to south-west and are aligned parallel to the main Caledonian structural grain and accretionary tract boundaries (GSNI, 1997; Anderson, 2004). Petrographical and geochemical studies have shown the Rathfriland and Cloghoge plutons to be normally zoned (more basic at their margins) and the Newry pluton to be reversely zoned (Neeson, 1984); however, to date no internal division of the plutons has been published. We have used the high-resolution Tellus aeromagnetic imagery, supported by new age dating, to map the structure of these plutons in greater detail than hitherto.

### Previous work

Doris Reynolds published prolifically on the rocks of the Newry Igneous Complex (Reynolds, 1934, 1936, 1943, 1946). Her research included detailed mapping of the intermediate-ultramafic rocks at its north-east end (Reynolds, 1934), which is now termed the Seconnell Complex (Fig. 11.1b). Reynolds proposed a non-magmatic granitisation model, in which Silurian greywackes were transformed *in situ* into granodiorite, with the ultramafic rocks representing a ‘basic front’ of ‘unwanted’ chemical elements, which migrated outwards. This hypothesis did not permit the presence of individual plutons and consequently embayments in the granodiorite/country rock contact were ignored (Fig. 11.1b).

Later work (Meighan and Neeson, 1979; Neeson, 1984) presented a magmatic interpretation in terms of three zoned, I-type or igneous-type (Chappell and White, 1974) granodiorite plutons. Petrogenetically, Meighan and Neeson (1979) proposed that the granodiorites originated principally by fractional crystallisation of more basic magmas (mainly at lower crustal depths) and that the ultimate, upper mantle progenitor might have been basaltic. Later, Meighan *et al.* (2003) reiterated this essentially upper mantle origin, invoking assimilation–fractional crystallisation as the explanation of any crustal component(s) in the granodiorites.

Various age constraints have been produced for the Newry Igneous Complex (see summary, Table 11.1), ranging from *c.*399 to 426 Ma depending on their vintage and the isotopic methods used.

TABLE 11.1. PREVIOUS RADIOMETRIC AGES FOR THE NEWRY IGNEOUS COMPLEX

Pluton	Age	Method/Comments	Reference
Rathfriland	399 ± 3 Ma	Rb-Sr whole rock/biotite regression	Meighan & Neeson (1979)
Newry	423 ± 7 Ma	U-Pb (zircon), SHRIMP, ANU, Canberra	Meighan <i>et al.</i> (2003)
Newry	426 ± 7 Ma	U-Pb (zircon), TIMS, GSC, Ottawa	Meighan <i>et al.</i> (2003)
Rathfriland	410 ± 1 Ma	U-Pb (titanite)/TIMS, GSC, Ottawa	Meighan <i>et al.</i> (2003)

## INTERPRETATION OF TELLUS GEOPHYSICAL DATA SETS

Examination of the Tellus data sets showed significant variations in the geophysical imagery of the Newry Igneous Complex (Fig. 11.2a, c). Fig. 11.2a shows the terrestrial gamma radiation presented in the form of a radiometric ternary image in which the combined intensities of radiometric uranium, thorium and potassium are depicted (Hodgson and Young, Chapter 2, this volume). The radiometric signal comes from radioactive emissions from only the upper  $\approx 30$  cm of soil and rock and can be used directly as an aid to geological mapping. Fig. 11.2c shows the total magnetic intensity, which is more complex and includes components from both shallow and deep magnetised bodies. The shape of a magnetic anomaly comprises positive and negative components, reflecting dip, strike and the direction of magnetisation. Fig. 11.2b and d shows the same figures with interpreted geological boundaries.

## ROCK SAMPLING AND ANALYTICAL METHODS

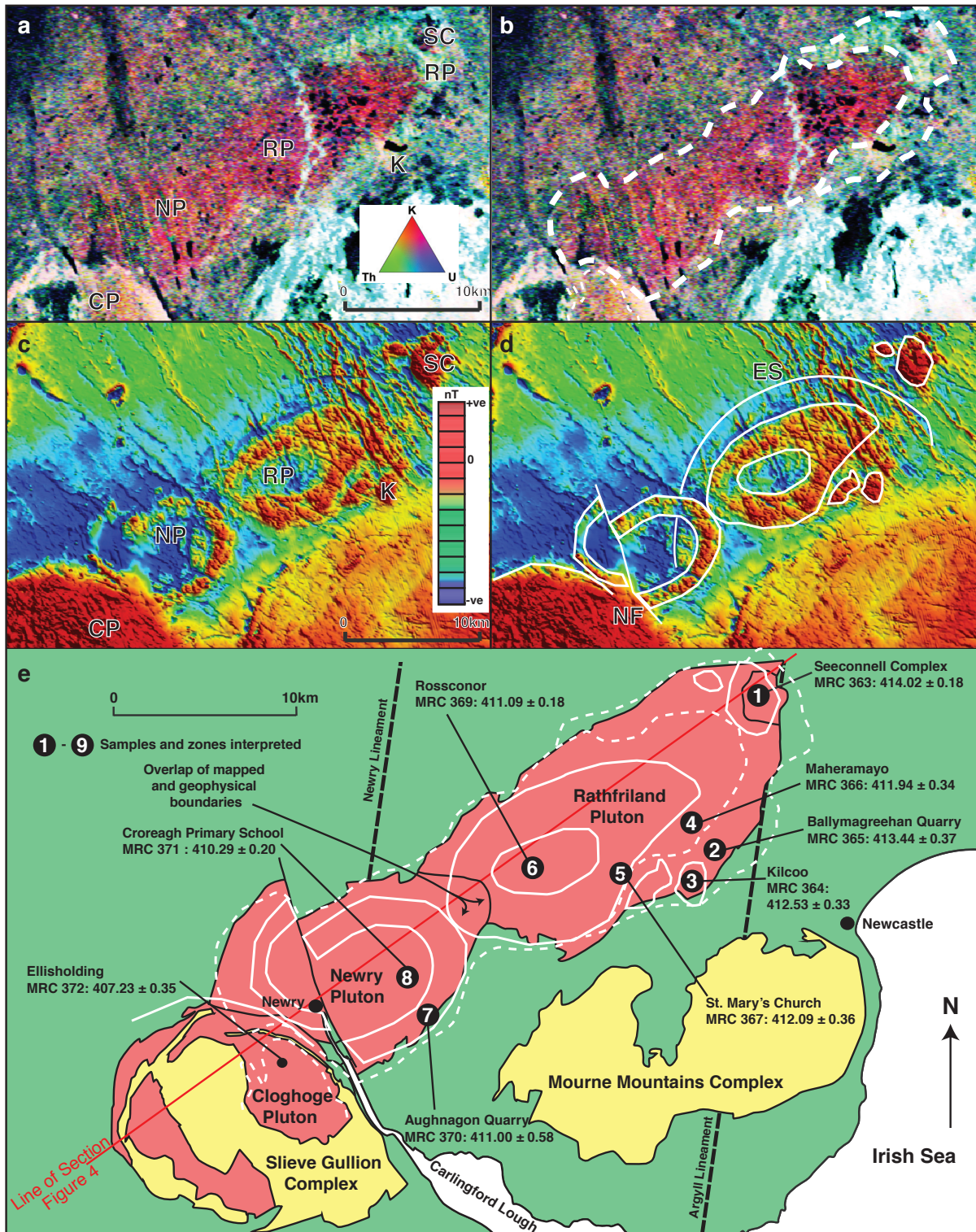
Nine sample sites were selected for dating according to the known geology, the geophysical zonation interpreted from Tellus imagery, and the availability of accessible outcrop (labelled 1–9, Fig. 11.2e). Rocks at these sites were dated by the well-established method of uranium–lead (U–Pb) chronology on zircon minerals, using the CA-ID-TIMS methodology at the NERC Isotope Geoscience Laboratories. Uranium–lead dates and uncertainties were calculated using the algorithms of Schmitz and Schoene (2007). A full account of the dating methods used can be found in the online technical appendix.

## RESULTS

### Tellus geophysics

Ternary radiometric data show the Newry pluton and the south-western part of the Rathfriland pluton (NP and RP on Fig. 11.2a) to be relatively rich in potassium compared with the north-eastern area of the Rathfriland pluton, which is predominantly thorium-elevated. Anomalies within the latter include the intermediate-ultramafic Seeconnell Complex (SC on Fig. 11.2a), which shows a potassium-elevated signal. The intermediate body in the vicinity of Kilcoo (K on Fig. 11.2a) also shows a mixed potassium–thorium–uranium signal. When the mapped boundary of the Rathfriland pluton (GSNI, 1997) is compared with the thorium elevated zone (Fig. 11.2e), a close match is observed along the north-western margin, while on the south-eastern margin there is a mismatch, with the interpreted thorium elevated zone extending 1–2 km towards the southeast. This mismatch is accounted for by glacial carryover of thorium elevated rock debris and is consistent with published glacial flow paths (Greenwood and Clark, 2008). It is also consistent with the principal component analysis of Tellus soils data (Dempster *et al.*, 2013), which shows high element loading of thorium in the Tellus data set to the south-east. The radiometric signature of the Cloghoge pluton (CP on Fig. 11.2a) is affected by the Palaeogene

Figure 11.2. (a) Tellus radiometrics image. (b) Radiometrics with interpretation. (c) Tellus magnetic image (reduced to pole). (d) Magnetics with interpretation. (e) Linework interpreted from magnetics and radiometrics superimposed on existing bedrock geology with geophysical zones and samples sites named and labelled (1–9). The new U–Pb dates are shown with calculated errors. Postulated traces of the Newry and Argyll lineaments are also shown (after Cooper *et al.*, 2013).



Slieve Gullion intrusions (Cooper and Johnston, 2004b); however, the central portion is potassium-rich, but with more thorium than seen in the Newry or Rathfriland plutons.

Magnetic imagery (Fig. 11.2c and d) reveals striking concentric zones of positive and negative magnetic signatures inside the Newry and Rathfriland plutons, and also defines the positive intermediate-ultramafic bodies of Kilcoo and the Seeconnell Complex. Comparison of the positive magnetic rings with the mapped boundaries of the Newry and Rathfriland plutons reveals another mismatch, such that the ring inside the Rathfriland pluton appears to overlap with the mapped geological boundary of the Newry pluton (Fig. 11.2e). The strongly positive magnetic signature of the Cloghoge pluton (Fig. 11.2c) is thought to have been caused by rocks (gabbro and dolerite) of the Slieve Gullion Complex (Fig. 11.1b).

Both the Newry and Cloghoge plutons are offset dextrally by NNW–SSE trending Cenozoic faults. The most obvious of these is the Newry Fault (NF in Figure 11.2d) which cuts the Newry pluton and displaces the positively magnetised ring by *c.*2.5 km (Cooper *et al.*, 2012). The magnetic image also reveals an elliptical structure that cuts country rock and the north-eastern part of the Rathfriland pluton, and possibly the western part of the Newry pluton, and is therefore younger (ES in Figure 11.2d). This may reflect a previously unrecognised cone sheet similar to that exposed at Glassdrumman on the east County Down coast (Fig. 11.1b), which is associated with granites of the Palaeogene Mourne Mountains Complex.

TABLE II.2. SUMMARY OF NEW U-Pb AGES FOR THE NEWRY IGNEOUS COMPLEX

	Pluton/ Complex	IGR	Zone	$^{206}\text{Pb}/^{238}\text{U}$ (Ma)	$\pm (2\sigma, \text{abs})$	MSWD*	<i>n</i>
MRC 363	Seeconnell	332430 342350	1	414.02	0.18	1.20	5 of 6
MRC 365	Rathfriland	330450 335450	2	413.44	0.37	1.30	4 of 5
MRC 364	Kilcoo	327820 333150	3	412.53	0.33	2.10	3 of 5
MRC 366	Rathfriland	329270 336940	4	411.94	0.34	0.57	4 of 5
MRC 367	Rathfriland	324830 333600	5	412.09	0.36	1.70	4 of 5
MRC 369	Rathfriland	320060 333950	6	411.09	0.18	0.71	4 of 7
MRC 370	Newry	314390 325150	7	411.00	0.58	3.50	4 of 4
MRC 371	Newry	312420 329820	8	410.29	0.20	1.60	5 of 6
MRC 372	Cloghoge	307860 322510	9	407.23	0.35	–	1 of 13

\*Mean square weighted deviation.

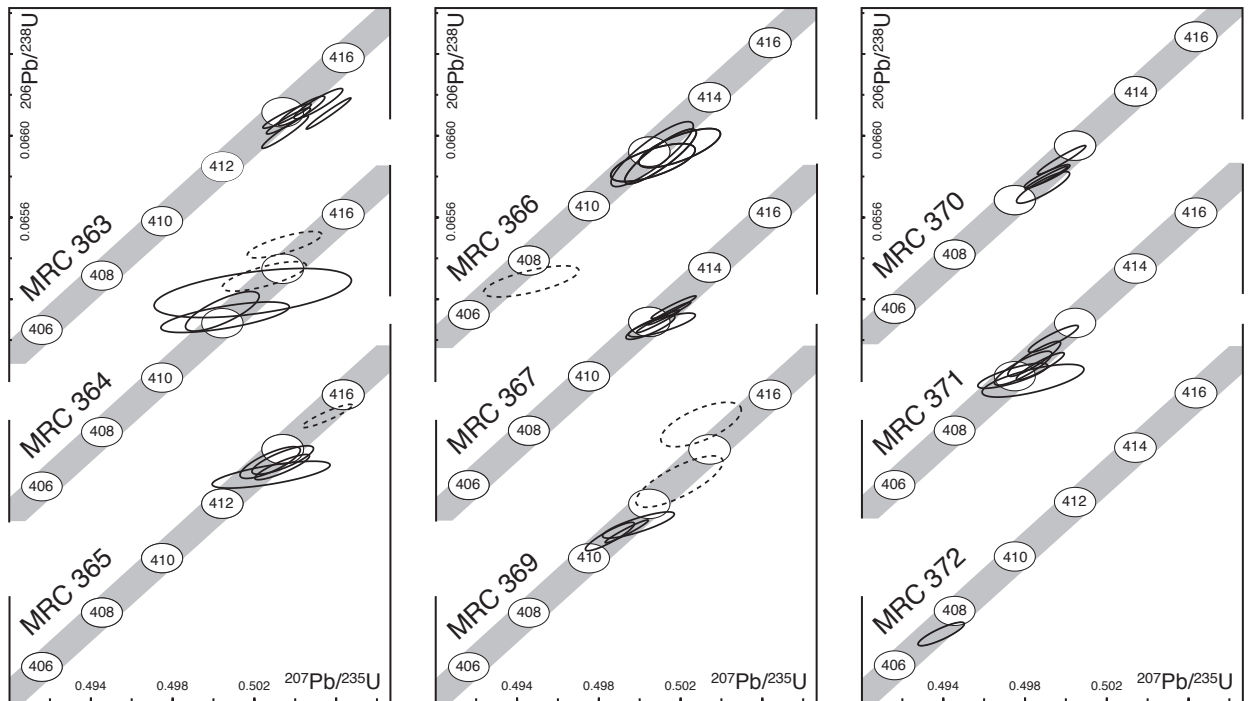
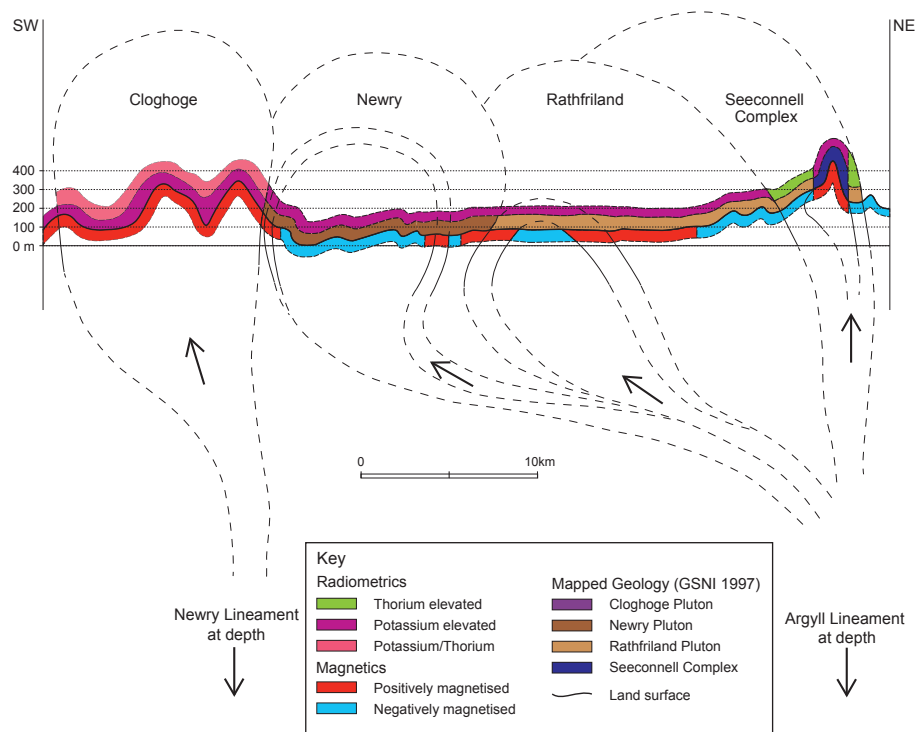


Figure 11.3. Stacked concordia plots for nine new U-Pb zircon age constraints for the Newry Igneous Complex.

### U-Pb geochronology

Nine new U-Pb TIMS zircon age dates have been determined for the Newry Igneous Complex at *c.*414–407 Ma. Analyses, summary data and concordia plots are shown in Table 11.2 and Fig. 11.3. The concordia plots demonstrate the concordant nature and tight clustering of the majority of the analyses performed, while the summary table includes the interpreted age in millions of years (Ma) and the calculated errors. A comprehensive data table (Table 11.3) for the U-Pb analyses performed can be found in the online technical appendix.

From the nine U-Pb age constraints presented in the summary (Table 11.2), the following can be said of the Newry Igneous Complex: (1) the entire complex was intruded over at least a *c.*7 myr period during the Lower Devonian; (2) the age of the plutons youngs from north-east to south-west (Fig. 11.2e); (3) the Seeconnell Complex is the oldest dated part of the Newry Igneous Complex; (4) within the Rathfriland and Newry plutons ages decrease from the margins to the centre of each pluton; (5) most of the magma (based on aerial extent of exposed plutons) was emplaced during the first *c.*4 myrs forming the Rathfriland and Newry plutons; (6) large age differences are also apparent within individual plutons, particularly the Rathfriland pluton; (7) the Cloghoge pluton may have been intruded some 2–3 myrs after the other plutons that make up the complex, although only one date has been acquired from the centre of this pluton and so the time gap could be less.



## DISCUSSION

The post-subduction Newry Igneous Complex was intruded from *c.*414 to 407 Ma during a period of orogen-wide sinistral transtension (or extensional shearing) during the Lower Devonian from *c.*420 to 400 Ma (see Brown *et al.*, 2008; Soper and Woodcock, 2003; Dewey and Strachan, 2003).

The progressive north-east to south-west younging of the complex is important because it shows that the siting or accommodation of magma in the crust moved to the south-west over the period of emplacement. However, it is also clear that intrusion occurred in stages, with most of the magma being emplaced during the first *c.*4 myrs into the Rathfriland and Newry plutons. The reason for emplacement being seemingly more rapid between *c.*414 and 410 Ma is not fully understood and according to the work of Brown *et al.* (2008) should not relate to a change in regional scale tectonic regime, which is considered to be trans-tensional throughout the whole period of intrusion. Significant differences of age between the geophysically recognised zones indicate that plutons were emplaced as a series of magma pulses.

Figure 11.4 presents a schematic cross-section through the Newry Igneous Complex from south-west to north-east. It integrates the surface mapped geology and locations of radiometrics and magnetic anomalies on a topographic profile. The contacts between mapped plutons are from the bedrock Geological Map of Northern Ireland (GSNI, 1997).

Figure 11.4. Schematic cross-section through the Newry Igneous Complex that integrates mapped geological boundaries and those interpreted from Tellus geophysics. The section is drawn on an accurate but simplified topographic profile.

The radiometric or magnetised zones correspond to those drawn on Fig. 11.2e. Radiometrics measure properties to  $\leq 30$  cm, which constrains the position of a geological contact to the surface, for example by the change from thorium to potassium elevated granodiorite in the Rathfriland pluton (zones 2 and 4 in Fig. 11.2e). However, magnetics ‘see’ farther into the earth and an anomaly at the surface will represent a sloping body or volume thinner than the surface expression. The interpretation is aided further by the following observations. There is a mismatch between the mapped geological boundary of the Newry and Rathfriland plutons and the magnetic anomalies contained within them (see Fig. 11.2e). This can be explained by a steep inward dipping contact of the Newry against the Rathfriland pluton and this suggests that the younger Newry pluton was emplaced above the south-western end of the Rathfriland pluton. The age of the inner, negatively magnetised, zone of the Rathfriland pluton is very similar to the outer part of the Newry (Fig. 11.2e), which may point towards a lateral migration of the site of pluton intrusion as depicted (Fig. 11.4). At the north-eastern end of the Rathfriland pluton, the positive anomaly appears to become broader than on its south-western end (Fig. 11.2c, d), suggesting either a widening of the zone of positively magnetised rock or a more shallow dipping contact between positively and negatively magnetised rock (Fig. 11.4). Both the Newry and Cloghoge plutons are offset dextrally by NNW–SSE trending Cenozoic faults. The most obvious of these is the Newry Fault (Fig. 11.1b), which cuts the Newry pluton and displaces the positively magnetised ring by *c.* 2.5 km (Cooper *et al.*, 2012). The even displacement of the positive anomaly along the length of the fault supports the idea that the contact of the pluton with country rock is steeply inclined.

Cooper *et al.* (2013) proposed a series of deep crustal structures, or lineaments across the north of Ireland that are based on the locations of igneous bodies, mineral deposits and regionally significant faults and strike swings. The exact nature of these lineaments, other than representing long lived, deep-seated faults, is not known, but two separate structures are proposed to pass through the Newry Igneous Complex (Figs 11.2e and 11.4). These are the Newry Lineament, which passes through the eastern part of the Cloghoge pluton, and the Argyll Lineament, which passes through the Seeconnell Complex in the very north-east of the Newry Igneous Complex. It is possible that magma initially ascended through the Argyll Lineament and then later through the Newry Lineament as accommodation space developed at higher levels from north-east to south-west.

In assessing the geothermal potential of Irish granites, Willmot Noller (2015) found a wide range of heat production characteristics in the Caledonian granites; some show high levels similar to those of the Palaeogene Mourne Mountains Complex but most, including the Newry Igneous Complex, show low–intermediate values. While the Newry Igneous Complex offers little potential for energy exploration, these results may contribute to understanding the emplacement mechanisms and the gross structure of other complexes with greater economic potential.

## CONCLUSIONS

This chapter presents the findings of two significant studies that have increased our understanding of the intrusion history of the Newry Igneous Complex: (1) the high resolution Tellus geophysical survey of Northern Ireland, which has revealed previously unseen zonation of the complex; and (2) high-precision U-Pb zircon dating of nine samples that provides a robust set of age constraints (*c.*414–407 Ma). The value of this study is demonstrated through the proposal of a subsurface model which is an important step towards understanding the shape and mechanisms of intrusion. Although the Newry Igneous Complex is not prospective for minerals or geothermal energy, this illustration of how Tellus data, with geological mapping and age dating, enable a better subsurface understanding of the pluton shape and emplacement can inform investigation of other more prospective plutons and complexes.

## ACKNOWLEDGEMENTS

This work and publication was made possible through a combination of Northern Ireland Department of Enterprise Trade and Investment funding and a joint Birmingham and SUERC NERC funded PhD. The GSNI Tellus Team and Adrian Walker (BGS) are thanked for assistance with interpretation of the geophysical imagery. Steve Noble, Paul Lyle and Tony Bazley are thanked for undertaking reviews. Alex Donald and Hugh Crilly are thanked for assistance with diagrams. MRC publishes with permission of the Executive Director of the British Geological Survey (NERC).

## REFERENCES

- Anderson, T.B., 2004 'Southern Uplands – Down–Longford Terrane', in W.I. Mitchell (ed.), *The Geology of Northern Ireland: Our Natural Foundation*. Second edition, 41–60. Belfast. Geological Survey of Northern Ireland.
- Beamish, D., Kimbell, G.S., Stone, P. and Anderson, T.B., 2010. 'Regional conductivity data used to reassess Early Palaeozoic structure in the Northern Ireland sector of the Southern Uplands – Down–Longford terrane', *Journal of the Geological Society*, 167, 649–57.
- Brown, P.E., Ryan, P.D., Soper, N.J. and Woodcock, N.H., 2008 'The Newer Granite problem revisited: a transtensional origin for the Early Devonian Trans-Suture Suite', *Geological Magazine*, 145, 2, 235–56.
- Chappell, B.W. and White, A.J.R., 1974 'Two contrasting granite types', *Pacific Geology* 8, 173–4.
- Condon, D., Schoene, B., Bowring, S., Parrish, R., McLean, N., Noble, S. and Crowley, Q. 2007, 'EARTHTIME: isotopic tracers and optimized solutions for high-precision U–Pb ID-TIMS geochronology', *Eos, Transactions, American Geophysical Union*, 88
- Cooper, M.R., Anderson, H., Walsh, J.J., Van Dam, C.L., Young, M.E., Earls, G. and Walker, A., 2012 'Palaeogene Alpine tectonics and Icelandic plume-related magmatism and deformation in Ireland', *Journal of the Geological Society*, 169, 29–36. Available at <http://nora.nerc.ac.uk/16421/>. <http://dx.doi.org/10.1144/0016-76492010-182>.
- Cooper, M.R., Crowley, Q.G., Hollis, S.P., Noble, S.R. and Henney, P.J., 2013 'A U-Pb age for the Late Caledonian Sperrin Mountains minor intrusions suite in the north of Ireland: timing of slab-breakoff in the Grampian terrane and the significance of long-lived deep crustal linea-

- ments', *Journal of the Geological Society*, 170, 603–14. Available at <http://nora.nerc.ac.uk/503145/>  
<http://dx.doi.org/10.1144/jgs2012-098>.
- Cooper, M.R. and Johnston, T.P., 2004a 'Late Palaeozoic Intrusives', in W.I. Mitchell (ed.), *The Geology of Northern Ireland: Our Natural Foundation*. Second edition, 61–8. Belfast. Geological Survey of Northern Ireland.
- Cooper, M.R. and Johnston, T.P., 2004b 'Palaeogene intrusive igneous rocks', in W.I. Mitchell (ed.), *The Geology of Northern Ireland: Our Natural Foundation*. Second edition, 179–98. Belfast. Geological Survey of Northern Ireland.
- Crowley, J.L., Schoene, B. and Bowring, S.A., 2007 'U-Pb dating of zircon in the Bishop Tuff at the millennial scale', *Geology*, 35, 12, 1123–6.
- Dempster, M., Dunlop, P., Scheib, A. and Cooper, M.R., 2013 'Principal component analysis of geochemistry of soils developed on till in Northern Ireland', *Journal of Maps*, 9, 3, 373–89. Available at <http://nora.nerc.ac.uk/503933/>. <http://dx.doi.org/10.1080/17445647.2013.789414>.
- Dewey, J.F. and Strachan, R.A., 2003 'Changing Silurian–Devonian relative plate motions in the Caledonides: sinistral transtension to sinistral transtension', *Journal of the Geological Society*, 160, 219–29.
- Greenwood, S.L. and Clark, C.D., 2008 'Subglacial bedforms of the Irish Ice Sheet'. *Journal of Maps*, 4, 1, 332–57.
- GSNI, 1997 *Northern Ireland. Solid Geology* (map, second edition). 1:250,000. Keyworth, UK. British Geological Survey.
- Jaffey, A.H., Flynn, K.F., Glendenin, L.E., Bentley, W.C. and Essling, A.M., 1971 'Precision measurements of half-lives and specific activities of  $^{235}\text{U}$  and  $^{238}\text{U}$ ', *Physics Reviews*, C4, 1889–906.
- Mattinson, J. M., 2005 'Zircon U-Pb chemical abrasion ("CA-TIMS") method: Combined annealing and multi-step partial dissolution analysis for improved precision and accuracy of zircon ages', *Chemical Geology*, 220, 1–2, 47–66.
- Meighan, I.G., Hamilton, M.A., Gamble, J.A., Ellam, R.M. and Cooper, M.R., 2003, 'The Caledonian Newry Complex, north-east Ireland: new U-Pb ages, a subsurface extension and magmatic epidote'. 46th Irish Geological Research Meeting, abstract. *Irish Journal of Earth Sciences*, 21, 156–7.
- Meighan, I.G. and Neeson, J.C., 1979 'The Newry Igneous Complex, County Down' in A.L. Harris, C.H. Holland and B.E. Leake (eds), *The Caledonides of the British Isles – Reviewed*. Special Publication No. 8, 717–22. London. Geological Society of London.
- Neeson, J.C., 1984, 'Petrology and geochemistry of the Newry complex'. Unpublished PhD thesis, Queen's University Belfast.
- Reynolds, D.L., 1934 'The eastern end of the Newry Igneous Complex', *Quarterly Journal of the Geological Society of London*, 90, 585–636.
- Reynolds, D.L., 1936 'The two monzonitic series of the Newry complex', *Geological Magazine*, 73, 337–64.
- Reynolds, D.L., 1943 'Granitization of hornfelsed sediments in the Newry granodiorite of Groughwood Quarry, Co. Armagh', *Proceedings of the Royal Irish Academy*, 48, Section B, No. 11, 230–67.
- Reynolds, D.L., 1946 'The sequence of geochemical changes leading to granitization', *Quarterly Journal of the Geological Society*, 102, 389–446.
- Schmitz, M.D. and Schoene, B., 2007 'Derivation of isotope ratios, errors and error correlations for U-Pb geochronology using  $^{205}\text{Pb}$ - $^{235}\text{U}$ -( $^{233}\text{U}$ )-spike isotope dilution thermal ionization mass spectrometric data', *Geochemistry, Geophysics, Geosystems* 8, Q08006.
- Soper, N.J. and Woodcock, N., 2003 'The lost Lower Old Red Sandstone of England and Wales: a record of post Iapetan flexure and Early Devonian transtension', *Geological Magazine*, 140, 627–47.
- Willmot Noller, N.M., Daly, J.S. and the IREITHERM team, 2015 'The contribution of radiogenic heat production studies to hot dry rock geothermal resource exploration in Ireland', in *Proceedings World Geothermal Congress*, April 2015. Melbourne, Australia.

### U-Pb geochronology

Zircons were analysed using CA-ID-TIMS methodologies employed at NERC Isotope Geoscience Laboratory (NIGL). Zircons were subject to a modified chemical abrasion pre-treatment for the effective elimination of Pb-loss (Mattinson 2005); and (2) the accuracy of the  $^{238}\text{U}/^{206}\text{Pb}$  dates presented herein are controlled by the gravimetric calibration of the EARTHTIME U-Pb tracer (ET535) employed in this study and the determination of the  $^{238}\text{U}$  decay constant (Condon *et al.* 2007; Jaffey *et al.* 1971).

Fragments/single zircons were placed in a muffle furnace at  $\sim 900$  °C for  $\sim 60$  hours in quartz dishes before being photographed. Crystals were then transferred to 300  $\mu\text{l}$  Teflon FEP microcapsules and 120  $\mu\text{l}$  of 29 M HF and  $\sim 25$   $\mu\text{l}$  of 30%  $\text{HNO}_2$  were added. Microcapsules were placed in a Parr vessel, and leached at 180 °C for 12–14 hours. The fractions were then removed and rinsed in ultrapure  $\text{H}_2\text{O}$ , fluxed at  $\sim 80$  °C on a hotplate for an hour in 6 M HCL, ultrasonically cleaned for another hour and then put back on a hot plate for  $\sim 30$  minutes. HCl solutions were then removed and the zircons rinsed again with ultrapure acetone and  $\text{H}_2\text{O}$ , and spiked with the ET535 tracer solution. Zircons were dissolved using Parr vessels in 120  $\mu\text{l}$  of 29 M HF with  $\sim 25$   $\mu\text{l}$  of 30%  $\text{HNO}_3$  at 220 °C for 48 hours and were then dried to fluorides on a 120 °C hotplate. Salts were re-dissolved in 6  $\mu\text{l}$  of 3.1 M HCl and ready for column chemistry. Zirconium, Hafnium, and rare earth element washes were saved for future work. U and Pb were loaded as one on a single Re filament using a silica-gel/phosphoric acid combination (Gerstenberger and Haase 1997). Isotope ratio measurements were performed at the Natural Environment Research Council Isotope Geology Laboratory (NIGL) on a Thermo-Electron Triton TIMS instrument equipped with a modified MassCom SEM that is effectively stable with a linear response effect, up to  $10^6$  counts/second, and thus allows for measurement of small Pb loads using a low noise amplifier for  $\text{UO}_2$ + analysis in static mode.

U-Pb dates and uncertainties were calculated using the algorithms of Schmitz and Schoene (2007), combined with a  $^{235}\text{U}/^{205}\text{Pb}$  ratio of 100.18 and  $^{233}\text{U}/^{235}\text{U}$  double spike ratio of 0.99464 for the ET535 tracer. All common Pb in the analyses was attributed to the blank and subtracted based on the isotopic composition and associated uncertainties analyzed over time. Errors for U-Pb dates are reported in the following format:  $\pm X(Y)[Z]$ , where X is the internal or analytical uncertainty in the absence of systematic errors (tracer calibration and decay constants), Y includes the quadratic addition of tracer calibration error (using a conservative estimate of the standard deviation of 0.1% for the Pb/U ratio in the tracer), and Z includes the quadratic addition of both the tracer calibration error and additional  $^{238}\text{U}$  decay constant errors of Jaffey *et al.* (1971). All analytical uncertainties are calculated at the 95% confidence interval. These  $^{238}\text{U}/^{206}\text{Pb}$  dates are traceable back to SI units via the gravimetric calibration of the EARTHTIME U-Pb tracer and the determination of the  $^{238}\text{U}$  decay constant (Jaffey *et al.*, 1971; Condon *et al.*, 2007).

**TABLE 11.3.** U-Pb DATA FOR ZIRCONS FROM THE NEWRY IGNEOUS COMPLEX

	Sample Parameters						Radiogenic Isotope Ratios								Isotopic Ages					
	Th	<sup>206</sup> Pb*	mol %	Pb*	Pb <sub>c</sub>	<sup>206</sup> Pb	<sup>208</sup> Pb	<sup>207</sup> Pb		<sup>207</sup> Pb		<sup>206</sup> Pb		corr.	<sup>207</sup> Pb		<sup>207</sup> Pb		<sup>206</sup> Pb	
Sample	U	x10 <sup>-13</sup> mol	<sup>206</sup> Pb*	Pb <sub>c</sub>	(pg)	<sup>204</sup> Pb	<sup>206</sup> Pb	<sup>206</sup> Pb	% err	<sup>235</sup> U	% err	<sup>238</sup> U	% err	coef.	<sup>206</sup> Pb	±	<sup>235</sup> U	±	<sup>238</sup> U	±
(a)	(d)	(e)	(e)	(e)	(e)	(f)	(g)	(g)	(h)	(g)	(h)	(g)	(h)		(i)	(h)	(i)	(h)	(i)	(h)
MRC 363																				
z1	0.746	28.8634	99.94%	565	1.36	32166	0.235	0.055156	0.078	0.503513	0.185	0.066209	0.122	0.952	418.11	1.75	414.08	0.63	413.35	0.49
z2	0.755	18.4818	99.93%	469	1.05	26714	0.238	0.055137	0.095	0.504317	0.184	0.066337	0.110	0.915	417.37	2.12	414.62	0.63	414.13	0.44
z3	0.763	12.9511	99.93%	434	0.80	24707	0.240	0.055118	0.090	0.503676	0.175	0.066276	0.098	0.941	416.59	2.00	414.19	0.60	413.76	0.39
z5	0.724	4.9293	99.51%	65	2.00	3735	0.228	0.055085	0.111	0.503607	0.191	0.066307	0.091	0.935	415.25	2.48	414.14	0.65	413.94	0.37
z6	0.778	14.8428	99.71%	112	3.56	6308	0.245	0.055191	0.100	0.505143	0.193	0.066381	0.114	0.917	419.56	2.23	415.18	0.66	414.39	0.46
z4	0.761	14.4473	99.79%	152	2.55	8575	0.240	0.055296	0.053	0.505645	0.177	0.066322	0.117	0.980	423.77	1.19	415.52	0.60	414.03	0.47
MRC 364																				
z3	0.819	1.1740	99.10%	36	0.87	2062	0.258	0.055047	0.204	0.501463	0.294	0.066070	0.149	0.768	413.72	4.55	412.69	1.00	412.51	0.59
z4	0.870	0.7035	98.98%	32	0.60	1810	0.273	0.054932	0.228	0.503484	0.295	0.066475	0.099	0.772	409.05	5.10	414.06	1.00	414.96	0.40
z7	1.173	0.3634	98.87%	31	0.34	1639	0.369	0.055039	0.265	0.503006	0.335	0.066282	0.110	0.732	413.48	5.92	413.74	1.14	413.78	0.44
z9	0.928	0.3108	97.89%	16	0.55	876	0.291	0.054979	0.443	0.500573	0.513	0.066034	0.115	0.684	410.98	9.90	412.09	1.74	412.29	0.46
z8	0.820	0.7345	90.87%	3	6.13	199	0.257	0.055005	0.711	0.501928	0.787	0.066182	0.184	0.508	412.01	15.90	413.01	2.67	413.18	0.74
MRC 365																				
z1	0.736	2.2039	99.49%	63	0.93	3601	0.231	0.055044	0.164	0.502781	0.240	0.066248	0.119	0.784	413.57	3.67	413.58	0.81	413.59	0.48
z3	0.753	0.6273	99.44%	57	0.29	3265	0.237	0.055131	0.142	0.503368	0.217	0.066220	0.094	0.873	417.10	3.18	413.98	0.74	413.42	0.38
z3	0.756	0.5541	97.84%	15	1.02	842	0.238	0.055110	0.404	0.502829	0.469	0.066174	0.101	0.711	416.26	9.02	413.62	1.59	413.14	0.40
z4	0.831	1.7169	99.55%	72	0.65	4007	0.261	0.055114	0.124	0.505574	0.198	0.066531	0.087	0.915	416.44	2.76	415.47	0.68	415.29	0.35
z5	0.790	0.7155	99.34%	49	0.39	2759	0.248	0.055098	0.171	0.503396	0.244	0.066263	0.107	0.800	415.80	3.83	414.00	0.83	413.68	0.43
MRC 366																				
z2	0.557	2.0692	99.40%	51	1.02	3089	0.175	0.055080	0.145	0.500993	0.286	0.065968	0.206	0.876	415.01	3.24	412.37	0.97	411.90	0.82
z3	0.473	1.5984	98.53%	20	1.97	1246	0.149	0.055070	0.263	0.500622	0.338	0.065932	0.143	0.676	414.58	5.88	412.12	1.14	411.68	0.57
z4	0.469	5.5589	98.88%	26	5.25	1614	0.147	0.055023	0.168	0.500583	0.329	0.065983	0.244	0.869	412.66	3.76	412.10	1.11	412.00	0.98
z5	0.588	4.0352	95.38%	6	16.25	392	0.185	0.055016	0.315	0.494660	0.386	0.065210	0.119	0.691	412.42	7.05	408.08	1.30	407.31	0.47
z9	0.557	1.6884	98.36%	18	2.32	1115	0.176	0.055140	0.240	0.501931	0.325	0.066020	0.147	0.730	417.45	5.35	413.01	1.10	412.21	0.59
MRC 367																				
z1	0.696	1.0872	98.98%	31	0.93	1778	0.219	0.055078	0.200	0.501062	0.266	0.065979	0.089	0.816	414.97	4.48	412.42	0.90	411.97	0.35
z2	0.551	2.4982	99.74%	117	0.54	6977	0.173	0.055051	0.100	0.501633	0.179	0.066087	0.085	0.960	413.84	2.23	412.81	0.61	412.62	0.34
z3	0.585	4.0600	99.82%	167	0.62	9866	0.184	0.055059	0.092	0.501416	0.172	0.066049	0.085	0.973	414.16	2.05	412.66	0.58	412.39	0.34
z4	0.931	4.3101	99.83%	195	0.61	10620	0.293	0.055039	0.092	0.500867	0.173	0.066001	0.086	0.967	413.43	2.07	412.29	0.59	412.09	0.34
z5	0.880	2.7829	99.80%	162	0.47	8916	0.277	0.055028	0.129	0.500497	0.195	0.065965	0.091	0.839	412.97	2.89	412.04	0.66	411.87	0.36
MRC 369																				
z3	0.409	3.8943	99.81%	160	0.59	9968	0.128	0.054962	0.092	0.500947	0.174	0.066104	0.087	0.970	410.19	2.06	412.34	0.59	412.73	0.35
z4	0.734	5.7571	99.84%	204	0.75	11710	0.231	0.055012	0.093	0.499355	0.173	0.065834	0.087	0.960	412.30	2.07	411.27	0.59	411.08	0.35
z9	0.445	3.3378	99.74%	117	0.71	7203	0.140	0.054948	0.112	0.498514	0.197	0.065800	0.107	0.893	409.62	2.51	410.70	0.66	410.89	0.43
z5	0.449	4.5472	97.65%	12	9.10	770	0.141	0.055044	0.233	0.501917	0.347	0.066134	0.193	0.771	413.52	5.21	413.00	1.18	412.91	0.77
z8	0.435	1.9053	99.68%	93	0.50	5780	0.136	0.054873	0.247	0.502977	0.320	0.066480	0.166	0.651	406.55	5.52	413.72	1.09	415.00	0.67
z9	0.495	3.4037	97.64%	12	6.85	767	0.156	0.055044	0.212	0.499909	0.288	0.065869	0.099	0.835	413.52	4.74	411.64	0.97	411.31	0.39
z10	0.734	5.7571	99.84%	204	0.75	11710	0.231	0.055012	0.093	0.499338	0.173	0.065831	0.086	0.963	412.30	2.07	411.25	0.58	411.07	0.34
MRC 370																				
z3	0.366	10.2935	99.45%	53	4.70	3316	0.115	0.054994	0.095	0.499780	0.194	0.065911	0.108	0.958	411.49	2.13	411.55	0.66	411.56	0.43
z7	0.374	2.9678	99.63%	80	0.90	5034	0.118	0.055034	0.124	0.498873	0.213	0.065745	0.119	0.868	413.09	2.78	410.94	0.72	410.56	0.47
z8	0.351	4.8456	99.79%	141	0.83	8912	0.111	0.054999	0.109	0.499070	0.183	0.065812	0.088	0.916	411.66	2.43	411.07	0.62	410.97	0.35
z10	0.346	3.8835	99.84%	184	0.51	11661	0.109	0.055003	0.089	0.499041	0.172	0.065804	0.086	0.976	411.82	2.00	411.05	0.58	410.92	0.34
MRC 371																				
z1	0.506	3.0099	99.71%	106	0.71	6448	0.159	0.055033	0.106	0.498738	0.192	0.065728	0.103	0.915	413.09	2.37	410.85	0.65	410.45	0.41
z2	0.657	2.6867	99.71%	108	0.65	6331	0.207	0.054962	0.112	0.498439	0.212	0.065773	0.132	0.891	410.24	2.50	410.65	0.72	410.72	0.53
z5	0.555	1.9413	99.61%	79	0.62	4769	0.174	0.054964	0.116	0.499376	0.200	0.065894	0.101	0.906	410.29	2.60	411.28	0.68	411.46	0.40
z7	0.618	0.9341	99.48%	60	0.40	3555	0.194	0.054949	0.138	0.497893	0.231	0.065716	0.128	0.859	409.71	3.08	410.28	0.78	410.38	0.51
z9	0.512	1.2083	97.31%	11	2.77	678	0.161	0.055067	0.335	0.498379	0.409	0.065640	0.124	0.696	414.46	7.48	410.60	1.38	409.92	0.49
z10	0.459	0.8583	99.01%	30	0.70	1869	0.144	0.054932	0.214	0.497389	0.281	0.065670	0.095	0.795	408.98	4.78	409.93	0.95	410.10	0.38
MRC 372																				
z1	0.527	4.4246	97.64%	13	8.88	768	0.169	0.054760	0.208	0.426802	0.723	0.056527	0.673	0.958	401.90	4.65	360.90	2.20	354.56	2.32
z2	0.524	2.2580	98.81%	25	2.25	1536	0.167	0.054835	0.170	0.452075	0.266	0.059794	0.140	0.821	404.96	3.81	378.73	0.84	374.45	0.51
z3	0.423	3.6157	99.33%	44	2.01	2737	0.134	0.054857	0.127	0.472130	0.214	0.062421	0.110	0.886	405.88	2.85	392.66	0.70	390.42	0.42
z4	0.483	2.7688	97.63%	12	5.59	764	0.156	0.054794	0.216	0.418313	0.327	0.055370	0.179	0.788	403.24	4.84	354.84	0.98	347.49	0.61
z5	0.420	1.9152	99.01%	30	1.58	1851	0.132	0.054816	0.169	0.477239	0.245	0.063144	0.101	0.842	404.20	3.77	396.18	0.80	394.80	0.39
z6	0.705	5.7356	98.86%	27	5.51	1586	0.223	0.054968	0.128	0.478922	0.213	0.063191	0.093	0.946	410.45	2.86	397.33	0.70	395.08	0.36
z7	0.456	4.3161	97.17%	10	10.43	641	0.146	0.054773	0.226	0.434341	0.301	0.057512	0.102	0.807	402.43	5.07	366.25	0.93	360.57	0.36
z1	0.606	2.4639	99.25%	41	1.54	2439	0.191	0.054843	0.158	0.481730	0.226	0.063706	0.087	0.859	405.36	3.53	399.26	0.75	398.21	0.33
z4	0.666	5.2136	99.89%	288	0.47	16780	0.210	0.054941	0.120	0.493880	0.187	0.065197	0.089	0.858	409.37	2.68	407.55	0.63	407.23	0.35
z1	0.349	1.8628	99.76%	120	0.37	7635	0.110	0.054901	0.120	0.478144	0.192	0.								

Unearthed: impacts of the Tellus surveys of the north of Ireland

First published in 2016 by the

Royal Irish Academy

19 Dawson Street

Dublin 2

[www.ria.ie](http://www.ria.ie)

Copyright © 2016 Royal Irish Academy

ISBN: 978-1-908996-88-6

The articles in this book are open access and distributed under the terms of the Creative Commons Attribution 4.0 licence, which permits unrestricted use, distribution and reproduction in any medium, provided the original authors and source are credited. To view a copy of this licence, visit <https://creativecommons.org/licenses/by/4.0/>



Except where noted:

Geological mapping for Northern Ireland / Tellus data are provided by the Geological Survey of Northern Ireland.

Geological mapping for Ireland / Tellus Border data are provided by the Geological Survey of Ireland.

Topographic mapping for Northern Ireland is derived from Land and Property Services Open Data and contains public sector information licensed under the Open Government Licence v3.0. (<http://www.nationalarchives.gov.uk/doc/open-government-licence/version/3/>).

Topographic mapping for Ireland is derived from Ordnance Survey of Ireland Open Data (<https://creativecommons.org/licenses/by/4.0/legalcode>).

While every effort has been made to contact and obtain permission from holders of copyright, if any involuntary infringement of copyright has occurred, sincere apologies are offered, and the owner of such copyright is requested to contact the publisher.

British Library Cataloguing-in-Publication Data. A catalogue record is available from the British Library.

Design: Alex Donald, Geological Survey of Northern Ireland.

Index: Brendan O'Brien.

Printed in Poland by L&C Printing Group.

# Table of Contents:

## **Prelim**

DOI: <https://doi.org/10.7486/DRI.b851k323d>

## **Chapter 1**

The Tellus geosciences surveys of the north of Ireland: context, delivery and impacts

DOI: <https://doi.org/10.7486/DRI.st74s528d>

## **Chapter 2**

The Tellus airborne geophysical surveys and results

DOI: <https://doi.org/10.7486/DRI.t148tx96z>

## **Chapter 3**

The Tellus geochemical surveys, results and applications

DOI: <https://doi.org/10.7486/DRI.t722wq645>

## **Chapter 4**

Stakeholder engagement for regional geoscientific surveying: the Tellus Border communications campaign

DOI: <https://doi.org/10.7486/DRI.w089fr763>

## **Chapter 5**

Mineral resources and Tellus: the essential balance

DOI: <https://doi.org/10.7486/DRI.wd37kb12s>

## **Chapter 6**

Gold exploration in the north of Ireland: new targets from the Tellus Projects

DOI: <https://doi.org/10.7486/DRI.wh24m696v>

## **Chapter 7**

Using soil geochemistry to investigate gold and base metal distribution and dispersal in the glaciated north of Ireland

DOI: <https://doi.org/10.7486/DRI.wm11n3806>

## **Chapter 8**

Critical metals for hightechnology applications: mineral exploration potential in the north of Ireland

DOI: <https://doi.org/10.7486/DRI.wp98p0649>

## **Chapter 9**

A natural laboratory for critical metals investigations in the Mourne Mountains granites

DOI: <https://doi.org/10.7486/DRI.cc08ww45f>

## **Chapter 10**

Geothermal potential of granitic rocks of the Mourne Mountains

DOI: <https://doi.org/10.7486/DRI.ff36jm09f>

## **Chapter 11**

Shape and intrusion history of the Late Caledonian Newry Igneous Complex, Northern Ireland

DOI: <https://doi.org/10.7486/DRI.2v248822m>

## **Chapter 12**

Using Tellus data to enhance targeting of volcanogenic massive sulphide mineralisation in the Tyrone Igneous Complex

DOI: <https://doi.org/10.7486/DRI.5x226w262>

## **Chapter 13**

The geological significance of electrical conductivity anomalies of the Ordovician- Silurian Moffat Shale Group, Northern Ireland

DOI: <https://doi.org/10.7486/DRI.6m31f4149>

## **Chapter 14**

Faults, intrusions and flood basalts: the Cenozoic structure of the north of Ireland

DOI: <https://doi.org/10.7486/DRI.90205h306>

## **Chapter 15**

Information for agriculture from regional geochemical surveys: the example of soil pH in the Tellus and Tellus Border data

DOI: <https://doi.org/10.7486/DRI.dv14c8060>

## **Chapter 16**

An ecohydrological investigation of wetlands in the border counties of Ireland: a framework for a holistic understanding of wetland systems

DOI: <https://doi.org/10.7486/DRI.hd775d90j>

**Chapter 17**

Assessing nutrient enrichment risk to groundwater-dependent ecosystems in the border counties of Ireland  
DOI: <https://doi.org/10.7486/DRI.k356pk18j>

**Chapter 18**

Mapping the terrestrial gamma radiation dose  
DOI: <https://doi.org/10.7486/DRI.k930rb86z>

**Chapter 19**

Soils and their radiometric characteristics  
DOI: <https://doi.org/10.7486/DRI.mp495t62g>

**Chapter 20**

Modelling in-house radon potential using Tellus data and geology to supplement inhouse radon measurements  
DOI: <https://doi.org/10.7486/DRI.ns06hm86z>

**Chapter 21**

Determining geochemical threshold values from the Tellus data sets: the examples of zinc and iodine|  
DOI: <https://doi.org/10.7486/DRI.r2087418g>

**Chapter 22**

Identification of the geochemical signatures of diffuse pollution in the Tellus Border soil data set, using source apportionment  
DOI: <https://doi.org/10.7486/DRI.wh24m698d>

**Chapter 23**

Stream sediment background concentrations in mineralised catchments in Northern Ireland: assessment of 'pressures' on water bodies in fulfilment of Water Framework Directive objectives  
DOI: <https://doi.org/10.7486/DRI.x633tf86g>

**Chapter 24**

Mapping metallic contamination of soils in the Lower Foyle catchment  
DOI: <https://doi.org/10.7486/DRI.9k42bv355>

**Chapter 25**

Refining the human health risk assessment process in Northern Ireland through the use of oral bioaccessibility data  
DOI: <https://doi.org/10.7486/DRI.9p29cr199>

**Chapter 26**

Combining environmental and medical data sets to explore potential associations between environmental factors and health: policy implications for human health risk assessments  
DOI: <https://doi.org/10.7486/DRI.9s16dn03n>

**Chapter 27**

Mapping a waste disposal site using Tellus airborne geophysical data  
DOI: <https://doi.org/10.7486/DRI.9w03fh87q>

**Chapter 28**

The use of aero-magnetics to enhance a numerical groundwater model of the Lagan Valley aquifer, Northern Ireland  
DOI: <https://doi.org/10.7486/DRI.9z90gd711>

**Chapter 29**

Carbon sequestration in the soils of Northern Ireland: potential based on mineralogical controls  
DOI: <https://doi.org/10.7486/DRI.b277h9556>

**Chapter 30**

Spatial distribution of soil geochemistry in geoforensics  
DOI: <https://doi.org/10.7486/DRI.b564j6392>

**End matter**

DOI: <https://doi.org/10.7486/DRI.bc38m007j>